



OASIS-3: IMAGING METHODS AND DATA DICTIONARY

VERSION 2.2 JULY 2022

Knight
ADRC

Alzheimer's Disease Research Center
WASHINGTON UNIVERSITY ST. LOUIS

 Washington
University in St. Louis
SCHOOL OF MEDICINE

MIR Mallinckrodt Institute
of Radiology



CONTENTS

Version 2.2 July 2022	1
Introduction & Contact Information.....	5
Access to OASIS-3	5
Data Use Agreement.....	6
OASIS Projects and Citations	7
Data Releases.....	7
Release 1.0: March 2018	7
Release 1.2: April 2018	7
Release 2.0: July 2022.....	7
Change Log Records.....	8
Using Central.XNAT.ORG	8
Github Resources.....	9
Data scripts: Download and Session Matching	9
Demographics	11
Table 1-2. Subject Demographics	11
OASIS File Description.....	11
MR Images	12
PET Images.....	12
TableS 3-6. OASIS-3 Imaging Summary.....	13
Figure 1 Longitudinal Imaging.....	14
MR Imaging.....	15
MR Scanners	15
Scanning Methods	15
DTI Imaging	15
Resting State SCans – Slice Timing.....	16
ASL Parameters.....	16

Post-Processed MRI: Volumetric Segmentation	16
Freesurfer	16
Processing Background	17
Quality Control MEasures	17
Analysis Considerations	17
Correcting subcortical and cortical volumes for head size	18
Instructions for normalization of MRI freesurfer-derived cortical volumes	18
Additional Regional Calculations	19
MR Scanner Comperison: Siemens TIM Trio 3T and Siemens Biograph 3T mMR	19
PET Imaging	21
PET Scanners	21
HR+ Image Notes (PIB and FDG)	21
Tracers	21
PIB	21
AV45	21
FDG	22
AV1451	22
Post-Processed PET: Pet Unified Pipeline (PUP)	22
PUP Variable Nomenclature	23
Partial Volume Correction	23
Alternative Reference Region	24
Amyloid PET Imaging Analysis	24
Cutoff Values for Amyloid Positivity	25
Centiloid Conversion for Amyloid PET	26
Tau PET Imaging (OASIS3_AV1451)	28
Braak Staging	28
Cutoff Values for Tau Positivity	29

Freesurfer Variables	30
PUP Variables.....	33
References.....	38

INTRODUCTION & CONTACT INFORMATION

OASIS-3 is the latest release in the *Open Access Series of Imaging Studies (OASIS)* that aimed at making neuroimaging datasets freely available to the scientific community. By compiling and freely distributing this multi-modal dataset, we hope to facilitate future discoveries in basic and clinical neuroscience. Previously released data for OASIS-Cross-sectional (Marcus et al, 2007) and OASIS-Longitudinal (Marcus et al, 2010) have been utilized for hypothesis driven data analyses, development of neuroanatomical atlases, and development of segmentation algorithms. OASIS-3 is a longitudinal neuroimaging, clinical, cognitive, and biomarker dataset for normal aging and Alzheimer's Disease.

The OASIS datasets hosted by central.xnat.org provide the community with open access to a significant database of neuroimaging and processed imaging data across a broad demographic, cognitive, and genetic spectrum an easily accessible platform for use in neuroimaging, clinical, and cognitive research on normal aging and cognitive decline. All data is available via www.oasis-brains.org.

OASIS-3 is a retrospective compilation of data for 1378 participants that were collected across several ongoing projects through the WUSTL Knight ADRC over the course of 30years. Participants include 755 cognitively normal adults and 622 individuals at various stages of cognitive decline ranging in age from 42-95yrs. All participants were assigned a new random identifier and all dates were removed and normalized to reflect days from entry into study. The dataset contains 2842 MR sessions which include T1w, T2w, FLAIR, ASL, SWI, time of flight, resting-state BOLD, and DTI sequences. Many of the MR sessions are accompanied by volumetric segmentation files produced through Freesurfer processing. PET imaging from different tracers, PIB, AV45, and FDG, totaling over 2157 raw imaging scans and the accompanying post-processed files from the Pet Unified Pipeline (PUP) are also available in OASIS-3. Additionally, 451 Tau PET sessions and post-processed PUP are now available for OASIS-3 subjects in a subproject 'OASIS-3_AV1451'.

ACCESS TO OASIS-3

Access to OASIS imaging, clinical, and biomarker data is available for access after completing the Data Use Agreement. Please log all data access requests using the online forms at www.oasis-brains.org.

- Data is available for access at <https://central.xnat.org>
- Further resources, including updated copies of this Data Dictionary, are available online at www.oasis-brains.org.
- Both OASIS-1 (OASIS: Cross-Sectional) and OASIS-2 (OASIS: Longitudinal) are available at www.oasis-brains.org/#data.
- CONTACT INFORMATION: oasis-brains@nrg.wustl.edu

DATA USE AGREEMENT

The OASIS data are distributed to the greater scientific community under the following terms:

1. You will not attempt to establish the identity of or make contact with any of the included human participants.
2. You will acknowledge the use of OASIS data and data derived from OASIS data when publicly presenting any results or algorithms that benefitted from their use. Papers, book chapters, books, posters, oral presentations, and all other printed and digital presentations of results derived from OASIS data should contain the following:
 - a. Acknowledgments: "Data were provided [in part] by OASIS [insert appropriate OASIS source info]"
 - i. OASIS: Cross-Sectional: Principal Investigators: D. Marcus, R. Buckner, J. Csernansky J. Morris; P50 AG05681, P01 AG03991, P01 AG026276, R01 AG021910, P20 MH071616, U24 RR021382
 - ii. OASIS: Longitudinal: Principal Investigators: D. Marcus, R. Buckner, J. Csernansky, J. Morris; P50 AG05681, P01 AG03991, P01 AG026276, R01 AG021910, P20 MH071616, U24 RR021382
 - iii. OASIS-3: Longitudinal Multimodal Neuroimaging: Principal Investigators: T. Benzinger, D. Marcus, J. Morris; NIH P50 AG00561, P30 NS09857781, P01 AG026276, P01 AG003991, R01 AG043434, UL1 TR000448, R01 EB009352. AV-45 doses were provided by Avid Radiopharmaceuticals, a wholly owned subsidiary of Eli Lilly.
 - iv. OASIS-3_AV1451: Principal Investigators: T. Benzinger, J. Morris; AW00006993. AV-1451 doses were provided by Avid Radiopharmaceuticals, a wholly owned subsidiary of Eli Lilly.
 - v. OASIS-4: Clinical Cohort: Principal Investigators: T. Benzinger, L. Koenig, P. LaMontagne
 - b. Citation: The specific publications that are appropriate to cite in any given study will depend on what OASIS data were used and for what purposes. An annotated and current list of OASIS publications is available at <http://www.oasis-brains.org>.
 - i. OASIS: Cross-Sectional: <https://doi.org/10.1162/jocn.2007.19.9.1498>
 - ii. OASIS: Longitudinal: <https://doi.org/10.1162/jocn.2009.21407>
 - iii. OASIS-3: Longitudinal Multimodal Neuroimaging: <https://doi.org/10.1101/2019.12.13.19014902>
 - iv. OASIS-4: Clinical Cohort: <https://doi.org/10.1016/j.nicl.2020.102248>
 - c. All proposed publications or presentations using Florbetapir F18 (AV45) and Flortaucipir F18 (AV1451) PET data must be submitted to Avid Radiopharmaceuticals for review and comment thirty days prior to such presentation or publication for review of intellectual property interests. See below for contact information and details.
 3. You agree to provide the Knight ADRC upon request with information on your use of OASIS data
 4. Failure to abide by these data use terms may result in termination of your right to access and use OASIS data.

AVID CONTACT INFO FOR FLORBETAPIR (AV45) PRESENTATIONS AND PUBLICATIONS

All proposed publications or presentations using Florbetapir F18 (AV45) or Flortaucipir F18 (AV1451) PET data must be submitted to Avid Radiopharmaceuticals for review and comment 30 days prior to such presentation or publication for review of intellectual property interests. Please reference OASIS-brains.org and Washington University (Drs. Morris and Benzinger) in your email.

- Contacts:
 - o Patricia Aldea Stevenson <stevenson@lilly.com>

OASIS PROJECTS AND CITATIONS

Each OASIS project should be used independently and not combined. Due to anonymization participants may be included in all three datasets (OASIS-1, OASIS-2, and OASIS-3) under unique IDs.

- OASIS-1: Cross-Sectional T1w MR images across the lifespan (ages 18-96) with dementia status (doi: [10.1162/jocn.2007.19.9.1498](https://doi.org/10.1162/jocn.2007.19.9.1498))
- OASIS-2: Longitudinal T1w MR images in older adults (ages 60-96) with dementia status (doi: [10.1162/jocn.2009.21407](https://doi.org/10.1162/jocn.2009.21407))
- OASIS-3: Longitudinal Multimodal Neuroimaging (ages 42-95) with dementia status (doi.org: 10.1101/2019.12.13.19014902)
- OASIS-4: Clinical Cohort: <https://doi.org/10.1016/j.nicl.2020.102248>

DATA RELEASES

RELEASE 1.0: MARCH 2018

Initial Longitudinal release of data

- 1098 Subjects (age 42-95)
- Neuroimaging:
 - o 2118 MR Sessions
 - 1912 Freesurfer processed outputs
- Clinical and Cognitive Measures:
 - o 6534 Longitudinal Clinical follow-up assessments
 - o Neuropsych Assessments
 - o 4089 NACC UDS2 Assessments

RELEASE 1.2: APRIL 2018

- o 1435 PET Sessions
 - 1352 PET Unified Pipeline processed outputs

RELEASE 2.0: JULY 2022

Updated longitudinal data to existing subjects and addition of new subjects.

- New subjects and longitudinal session
 - o 280 Subjects (age 42-100)
 - o Neuroimaging:

- 674 MR Sessions
 - 633 Freesurfer processed outputs
- 1472 CT session
- 550 PET Sessions
 - 493 PET Unified Pipeline processed outputs
- **Spreadsheets for download without using xnat tables**
- **UDS v2 and UDS v3**
- **Cohort Replication**
 - Option for storage of cohort data to replicate published results
- **OASIS3_AV1451**
 - Sub-project with Tau imaging on OASIS3 participants

CHANGE LOG RECORDS

- This is a changelog to track changes to the OASIS database.
 - https://github.com/NrgXnat/oasis-scripts/blob/master/OASIS_CHANGELOG.md

USING CENTRAL.XNAT.ORG

SEARCHING, REPORTING, AND DATA MINING:

- **Standard Search:** <https://wiki.xnat.org/documentation/how-to-use-xnat/using-the-standard-search>
- **Using the Advanced Search:** <https://wiki.xnat.org/documentation/how-to-use-xnat/using-the-standard-search/using-the-advanced-search>
- **Saving a Data Table as a Stored Search:** <https://wiki.xnat.org/documentation/how-to-use-xnat/using-the-standard-search/saving-a-data-table-as-a-stored-search>
- **How to Edit, Filter, and Join Tables:** <https://wiki.xnat.org/documentation/how-to-use-xnat/using-the-standard-search/how-to-edit-filter-and-join-data-tables>

DOWNLOADING DATA

- **How to Download Files via the XNAT REST API (*recommended*):**
<https://wiki.xnat.org/display/XAPI/How+To+Download+Files+via+the+XNAT+REST+API>
 - **Scripted Download Instructions:** The following shell script can be used to download large amounts of data from the OASIS-3 dataset on XNAT Central.
 - Create a CSV spreadsheet with a list of sessions to download (or download a CSV from XNAT Central)
 - Download the script: <https://github.com/NrgXnat/oasis-scripts>
 - Open a Terminal window (on Mac) or Command Line window (on PC / Linux)
 - To run the script and download data, you need to provide the following parameters:
 - <input_file.csv> - your list of sessions to download
 - <directory_name> - the path to your local download folder

- <xnat_central_username> - your username
 - <scan_type> - (optional) the type of scan or scans to download
- **How to Download non-imaging assessments**
 - Subject "[OAS data files](#)" contains an MR session ([OASIS3 data files](#)) that has all csv files.
 - 1. click on MR session
 - 2. select assessments you want to download
 - 3. bulk action Download
 - This "MR session" includes files for:
 - Demographics
- **How to Download Images from UI:** <https://wiki.xnat.org/documentation/how-to-use-xnat/how-to-download-image-data-from-xnat-projects>
- **Troubleshooting XNAT Java Applet Issues:** <https://wiki.xnat.org/documentation/how-to-use-xnat/image-session-upload-methods-in-xnat/troubleshooting-xnat-java-applet-issues>
 - UDS v2 and UDS v3 assessments
 - Psychometric variables
 - Image processing outputs (freesurfer, PUP, Centiloid)
 - json summary files
 - Data dictionaries
 - Data use agreement

GITHUB RESOURCES

DATA SCRIPTS: DOWNLOAD AND SESSION MATCHING

[HTTPS://GITHUB.COM/NRGXNAT/OASIS-SCRIPTS](https://github.com/NrgXnat/oasis-scripts)

DOWNLOAD SCANS

- This script downloads scans of a specified type and organizes the files.
 - https://github.com/NrgXnat/oasis-scripts#download_scansdownload_oasis_scanssh
- This script downloads scans from OASIS and organizes the files into Brain Imaging Data Structure (BIDS) format (See the [BIDS website](#) and the [BIDS file specification](#) for more details on the BIDS format).
 - <https://github.com/NrgXnat/oasis-scripts#downloading-mr-and-pet-scan-files-in-bids-format>

DOWNLOAD FREESURFER

- The scripts contained in the `freesurfer` folder can be used to download Freesurfer data and organize the files.
 - <https://github.com/NrgXnat/oasis-scripts#downloading-freesurfer-files>

DOWNLOAD PUP

- The scripts contained in the pup folder can be used to download PUP data and organize the files.
 - <https://github.com/NrgXnat/oasis-scripts#downloading-pet-unified-pipeline-pup-files>

SESSION MATCHUP

- This script takes in two OASIS-3 .csv formatted spreadsheets and matches up the sessions based on your requested days from entry distance requirements. This script requires R at least version 3.3.0 and the R data.table library minimum version 1.12.8. See the R-project website for more details on the R language and visit the R data.table library website for more details on the data.table library.
OASIS-3 data has been anonymized and dates have been eliminated from the data set. OASIS-3 instead uses "days from entry" to note when scan sessions and questionnaire sessions happen relative to each other. The "days from entry" variable is seen in OASIS-3 IDs for MR sessions, PET sessions, Freesurfer assessors, PUP assessors, and questionnaire sessions (such as ADRC Clinical Data entries or UDS form entries). At the end of each ID is a string d0000 where 0000 is the days since the subject's entry date into the study. A days from entry value of 0 means that this is the subject's first visit.
 - <https://github.com/NrgXnat/oasis-scripts#matching-up-session-data-by-days-from-entry>

DEMOGRAPHICS

TABLE 1-2. SUBJECT DEMOGRAPHICS

Table 1. Subject Demographics

	N	AGE	Right Handed
F	756	68.15 (43.2-95.6)	684
M	622	70.16 (42.5-91.7)	551
Total	1378	69.06 (42.5-95.6)	1235

Table 2. OASIS-3 Clinical Dementia Rating (CDR) Summary

		max CDR					
min CDR		0	0.5	1	2	3	Grand Total
0	755*	215	61	38	7	1076	
0.5		83	57	74	7	221	
>1			33	36	5	74	
Grand Total	755	298	151	154	19	1377	

*Unchanged CDR = 0 represents cognitively healthy population. List provided on Central

OASIS FILE DESCRIPTION

BIDS FILE SPECIFICATION

All MR and PET imaging files are converted to nifti format utilizing the BIDS format (Gorgolewski et al., 2016). This allows for standardized naming and file formats. Raw MR files, in DICOM or IMA format were converted to Nifti format using dcm2nii (DICOM=dcm2niix v1.0.20171017 and IMA=dcm2nii mriconrlx64-2013.06.12; Li et al., 2016). In addition to nifti files, a supplemental json file is included with additional acquisition header information, such as TR, TE, flip angle, and scanner model, that is absent from nifti headers.

Documentation on BIDS can be found here (<http://bids.neuroimaging.io/>).

*Nifti conversion was completed after volumetric processing that has two big implications.

- First, any new processing of T1 images through Freesurfer will result in different values as documented in FreeSurfer regarding file format changes.
- Second, the T1.mgz associated with the OASIS-3 Freesurfer processing is the result of dicom conversion to mgz and can be used in place of the T1w.nii file for comparative FreeSurfer processing.**

MR IMAGES

- anat
 - T1w
 - T2w
 - TSE (acq-TSE_T2w)
 - T2star
 - FLASH
 - Flair
 - Time of Flight (acq-TOF_angio)
- func
 - Task-rest_bold
 - ASL
- fmap
 - Fieldmap
- dwi
 - DWI
 - bvec (vector table)
 - bval (vector of b-values)
- swi
 - Magnitude (part-Mag_GRE)
 - Phase (part-Phase_GRE)
 - Minimum Intensity Projection (minIP)
 - SWI

PET IMAGES

- pet
 - acq-PIB_pet
 - acq-AV45_pet
 - acq-FDG_pet
 - acq-AV1451_pet* (*only in project: OASIS3_AV1451)

TABLES 3-6. OASIS-3 IMAGING SUMMARY

Table 3. OASIS-3 MR and PET Imaging Summary

OASIS-3 – Longitudinal Normal Aging and Alzheimer Disease											
		Subjects	MR	Freesufer	CT	PET	AV45	PIB	FDG	AV1451	PUP
2018 Release		1098	2168	1912	0	1607	491	999	117		1352
2022 Release		281	674	633	1472	550	290	250	10		493
Total OASIS-3		1379	2842	2545	1472	2157	781	1249	127		1845
OASIS3_AV1451 (restricted access)		451								449	434
OASIS3_AV1451_longitudinal (restricted access – WUSTL ADRC only)		79								81	72

Table 4. OASIS-3 MR Scan Type Inventory

Scan Type	T1w	T2w	FLAIR	Bold – Resting State	DTI	ASL	SWI	TOF	Fieldmap
OASIS-3									
1.5T MR	654	455	0	2	0	0	2	1	2
3.0T MR (Release 2018)	2734	3145	748	3640	2450	1113	1217	674	2922
3.0T MR (Release 2022)	728	450	633	1474	819	447	12	222	895
OASIS-4	1846	769	671	10	656	1	663	18	3

OASIS-3 – Longitudinal Normal Aging and Alzheimer Disease							
	Release 2018			Release 2022			Total
	HR+	PET/CT	PET/MR	HR+	PET/CT	PET/MR	
PIB	411	580	8	11	239		1249
AV45	1	23	467	2		288	781
FDG	117			10			127
Total	529	603	475	23	239	288	

Table 5. PET imaging inventory by scanner and tracer

Table 6. Post-processing Data Summary

	Post-Processed Data (Release 2018)	Post-Processed Data (Release 2022)
FreeSurfer		
5.0/5.1	211	0
5.3	1701	633
PUP	1352	493
PIB	935	228
AV45	417	265
FDG	0	0

FIGURE 1 LONGITUDINAL IMAGING

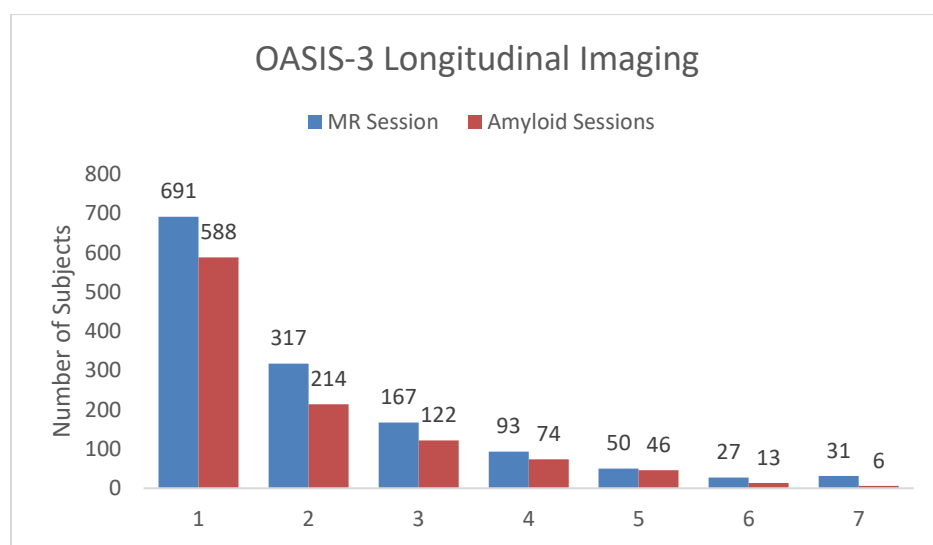


Figure 1. Longitudinal Imaging

MR IMAGING

MR SCANNERS

Data included in OASIS was collected on the following scanners. Scanner specific information is recorded in dataset_description.json for each MR scan session. *For manuscripts, select only the scanner(s) from which your subset of data were derived.*

- Siemens BioGraph mMR PET-MR 3T scanner (51010)
- Siemens TIM Trio 3T MR scanner (2 scanners) (35177 & 35248)
- Siemens Magnetom Vida 3T MR scanner (175614)
- Siemens Prisma_fit 3T MRI scanner (167047)
- Siemens Sonata 1.5T scanner (21926)
- Siemens Vision 1.5T scanner
- Siemens Avanto 1.5T scanner (26321)

SCANNING METHODS

- Participants were placed in the scanner head to foot while lying in the supine position.
- Head immobilization was done by placing small foam cushions between the head and the head coil.
- In many participants, a Vitamin E capsule was used to mark the left temple.
- For all scans a 16-channel head coil was used.
- Participants receiving simultaneous PET acquisition, on the BioGraph mMR were injected with tracer prior to initiation of MRI scanning
- Magnetom Vida scan sessions were converted to NIFTI format from enhanced DICOM format
- Note that not all subjects will have every type of image data.

DTI IMAGING

The OASIS-3 dataset includes 1205 DTI. All sequences include a *bvec and *bval file that includes information on the vectors and b-values as estimated through the dcm2niix conversion. These files are found in the BIDS folder associated with the DTI nifti. DTI sequences collected on Siemens scanners are known to have a variance of +/- 10%. Below is the standard vector table for Siemens 25-direction DTI.

VECTOR TABLE FOR 25 DIRECTIONS

```
CoordinateSystem = xyz
Normalisation = none
25 direction
0,1,2,3,4,5,6,7,8,9,10,11,12,13,14,15,16,17,18,19,20,21,22,23,24
-0.200000,-0.457663,-0.619678,-0.647200,-0.529196,-0.163313,-0.305531,-0.346410,-0.294225,-0.334708,-0.876353,-0.107041,-0.174797,-
0.222823,0.000000,0.000000,0.000000,0.231234,0.435890,0.489898,0.223607,0.365180,0.626649,0.723592,0.809004
0.000000,0.000000,0.000000,-0.420560,-0.529196,0.163313,0.305531,0.589382,-0.770361,0,-0.294691,0.000000,0.000000,-0.446071,-
0.815963,-0.142720,0.214080,-0.636606,-0.458295,0.515079,0.380445,0.365180,-0.407205,0.000000,0.000000
0,-0.174796,0.236674,0.21032,-0.529196,-0.163313,0.305531,0.112583,0,0.147328,-0.538023,0.685848,0.721758,-0.504234,-0.37368,-
0.56052,0.318265,-0.599959,0.674296,0.072672,-0.365180,0.203641,-0.525744,0.587803
```

RESTING STATE SCANS – SLICE TIMING

Resting state scans are labeled according to BIDS standard “task-rest”. Slice timing is included in the JSON when available. Some original DICOM files did not have slice timing info. [When slice timing information is unavailable use the ratio TR/#slices.](#)

ASL PARAMETERS

The following parameters are important for processing ASL images but were not extracted into the JSON files as part of the BIDS conversion.

Table 7. ASL Parameters by scanner

Scanner model	Software Version	TI1	TI2	Labeling Strategy	Slice Readout	Background Suppression
51010	syngo_MR_B18P	700	1900	PASL	46.0ms	None
51010	syngo_MR_B20P	700	1900	PASL	46.0ms	None
35177	syngo_MR_B17P	700	1900	PASL	36.4ms	None
35248	syngo_MR_B17P	700	1800	PASL	36.4ms	None
175614				PASL		

POST-PROCESSED MRI: VOLUMETRIC SEGMENTATION

Single T1w MRI images were processed through Freesurfer to provide volumetric MRI data and segmentations maps. These maps can be used for a variety of purposes such as determining cortical volumes or regions of interest (ROIs) for PET imaging.

FREESURFER

OASIS-3 is a retrospective project that required anonymization of all files. In order to anonymize FreeSurfer output the following were removed: dates, timestamps, QC staff, raw file paths, original directory paths, ID change, and removal of all logs. OASIS-3 provides volumetric values representing Surface Measures from the aparc.stats Freesurfer output file and Subcortical Segmentation from the aseg.stats Freesurfer output file. These can be downloaded in csv format. All additional files, t1.mgz, brainmasks, segmentations, surface maps, and regional statistics.

**Conversion to BIDS format was completed following FreeSurfer processing. Segmentation of nifti files will produce different values than segmentation completed on dicom files and is documented by FreeSurfer. Direct comparison to OASIS-3 FreeSurfer files should be done using the T1.mgz file.*

For a full description of Subcortical Segmentation and Surface Measures statistical variable see [list](#).

PROCESSING BACKGROUND

FreeSurfer (<http://surfer.nmr.mgh.harvard.edu/>) analyses involved cortical reconstruction and volumetric segmentation of T1 weighted images.

The technical details of these procedures are described in prior publications (Dale et al., 1999; Dale and Sereno, 1993; Fischl and Dale, 2000; Fischl et al., 2001; Fischl et al., 2002; Fischl et al., 2004a; Fischl et al., 1999a; Fischl et al., 1999b; Fischl et al., 2004b; Han et al., 2006; Jovicich et al., 2006; Segonne et al., 2004)). The processing pipeline included motion correction and segmentation of the subcortical white matter and deep gray matter volumetric structures on a T1 weighted image (Fischl et al., 2002), intensity normalization, registration to a spherical atlas which utilized individual cortical folding patterns to match cortical geometry across subjects (Fischl et al., 1999b), and parcellation of the cerebral cortex into units based on gyral and sulcal structure (Desikan et al., 2006).

All MRI sessions were processed through the FreeSurfer image analysis suite using Dell PowerEdge 1950 servers with Intel Xeon processors running CentOS 5.5 Linux.

- All 1.5T imaging data was reprocessed using FreeSurfer 5.0 or Freesurfer 5.1.
- All 3.0T MRI imaging data was reprocessed using FreeSurfer 5.3-HCP-patch.
- All data (1.5 and 3.0 T) have been corrected per the 2012 patch released by MGH.

QUALITY CONTROL MEASURES

Individuals responsible for processing imaging data are trained in the FreeSurfer quality control (QC) measures developed by the KARI Imaging Core. During the QC process, the rater will locate all FreeSurfer errors in the cortical parcellation and subcortical segmentation that meet a certain size based on the QC criteria below. An error that meets the QC criteria will require manual intervention (editing the FreeSurfer) and/or will fail quality control. There are two main types of FreeSurfer QC errors: inclusion and exclusion. Inclusion errors are identified as non-brain regions (dura, skull, etc.) that are being assessed as part of the brain and exclusion errors are identified as brain regions that are excluded from the cortical/subcortical classification. Generally, three attempts will be made to fix FreeSurfer QC errors if the error persists after performing edits. After the third attempt, the FreeSurfer will either pass with a note indicating that edits were performed or fail QC depending on the size of the error

OASIS-3 includes FreeSurfer output for sessions that were of quality “pass” or “pass with edits”.

FreeSurfer QC criteria is as follows:

- Dural inclusion, gray matter exclusion, sulcus inclusion, cerebellum inclusion will require edits if equal to or larger than 120 voxels (mm³).
- Cerebellum, subcortical and hippocampus segmentation exclusion will fail quality control if greater than 120 voxels (mm³). Before failing, other errors will be fixed if possible, which may fix segmentation exclusions.
- White matter exclusion will require edits if equal to or larger than 60 voxels (mm³).
- Lateral ventricle segmented incorrectly will require edits if equal to or larger than 300 voxels (mm³).

ANALYSIS CONSIDERATIONS

CORRECTING SUBCORTICAL AND CORTICAL VOLUMES FOR HEAD SIZE

It is suggested that all regions volumes should be corrected for head size (intracranial volume, ICV) in order to have correct comparisons. This does not apply to cortical thickness measures, as cortical thickness does not significantly vary with head size. The normalization process applies to each individual ROI and is sample specific. Please note if participants are removed from the data set the normalizations on the subcortical volumes will need to be re-run.

Note: Volume normalization must be repeated every time a subject is added or removed from the sample.

To test the consistency of FreeSurfer derived ICV, an analysis of the ICV estimate for each participant was performed on a longitudinal cohort (Figure 2). All participants had MRI scans using a 3T scanner and were processed with FreeSurfer 5.3. Within a participant, ICV can vary from baseline more than 5% with a mean subject standard deviation of 15.75 cm^3 . This variance should be taken into consideration when correcting subcortical and cortical volumes.

Relevant publication for the head-size correction:

Randy L. Buckner, Denise Head, Jamie Parker, Anthony F. Fotenos, Daniel Marcus, John C. Morris, and Abraham Z. Snyder A unified approach for morphometric and functional data analysis in young, old, and demented adults using automated atlas-based head size normalization: reliability and validation against manual measurement of total intracranial volume. *Neuroimage*, 2004.

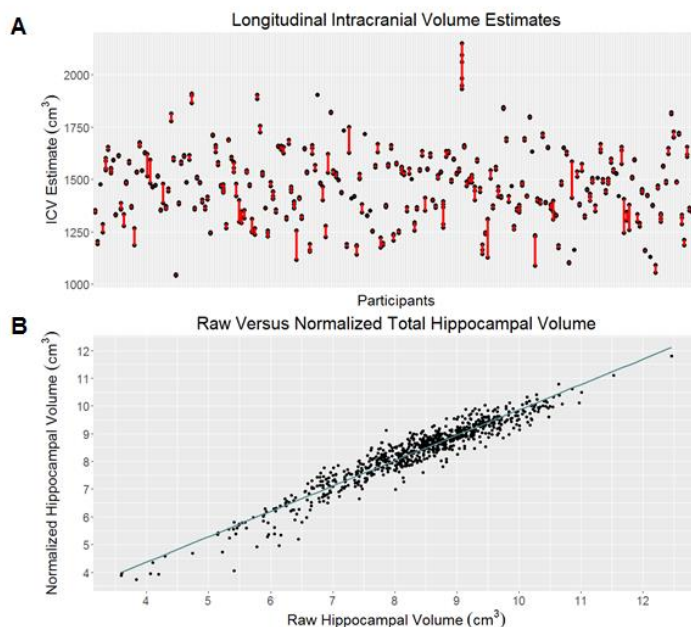


Figure 2 (A) ICV estimate for each participant in a longitudinal study. Each black circle represents an MR session and the red line represents a longitudinal participant. (B) The relationship between the raw hippocampal volume and the hippocampal volume normalized by ICV.

INSTRUCTIONS FOR NORMALIZATION OF MRI FREESURFER-DERIVED CORTICAL VOLUMES

Normalization Calculation:

1. Compute mean ICV for sample
2. Compute regression with ICV as independent variable and ROI as dependent variable to obtain B (NOT Beta) weight
3. Compute: **Normalized = raw volume – (B-weight * (ss ICV – mean ICV))**
[Note: "ss" = single subject's]
4. This procedure is repeated for each subcortical & cortical ROI volume the investigator is interested in.
 - a. These volumes can be found in the "aseg.stats" file.
 - b. We do not normalize the cortical thickness measures.

Table 8. Below shows a snapshot from the SPSS output for the linear regression. Use the B value highlighted in red for the correction factor. This will be repeated for each given ROI.

Model	Coefficients ^a					
	Unstandardized Coefficients			Standardized Coefficients	t	Sig.
	B	Std. Error	Beta			
1	(Constant)	2718.207	343.943		7.903	.000
	ICV	-1.513E-5	.000	-.008	-.068	.946

a. Dependent Variable: transtemp

ADDITIONAL REGIONAL CALCULATIONS

Regional FreeSurfer outputs can be combined to generate multiple global brain measures that researchers may find useful (see <https://surfer.nmr.mgh.harvard.edu/fswiki/MorphometryStats>):

- Whole Brain Volume = Cortex + CorticalWhiteMatter + SubCortGray
- Cortex = lhCortex + rhCortex
- CorticalWhiteMatter = lhCorticalWhiteMatterVol + rhCorticalWhiteMatterVol
- SubCortGray = summation of thalamus, caudate, hippocampus, amygdala, accumbens, ventral DC, substantia nigra (if there). This is a simple voxel count of structures identified as subcortical GM.
- Total Ventricular Volume = left and right lateral inferior lateral ventricles + 3rd + 4th + 5th ventricles

MR SCANNER COMPARISON: SIEMENS TIM TRIO 3T AND SIEMENS BIOGRAPH 3T MMR

In order to combine data from both the Siemens TIM Trio 3T MRI and the Siemens Biograph 3T mMR (PET MR), a direct correlation was performed in a subset of our participants. For the scanner validation, 69 participants with a mean age of 65.9 years (CDR 0-0.5) received both the Trio and mMR MRI within two weeks. Of the 69 participants, 67 participants were CN (CDR 0) and 2 participants had a diagnosis of mild symptomatic AD (CDR 0.5). FreeSurfer v5.1 was used to segment the brain into various regions of interest (ROI) for quantitative analysis.

For the left hippocampal volume as measured by Trio and the PET MR, the estimated concordance correlation coefficient (CCC) on the raw data is 0.83 with a 95% CI from 0.73 to 0.89, and after the standardization, the estimated CCC is 0.83 with a 95% CI from 0.74 to 0.90. For the right hippocampus volume as measured by Trio and the PET MR, the estimated CCC on the raw data is 0.79 with a 95% CI from 0.67 to 0.87, and after the standardization, the estimated CCC is still 0.79 with a 95% CI from 0.67 to 0.87.

Because of the two potential outliers on the hippocampal volumes data (Figure 3), rank-based CCC was performed on these measures. The rank-based CCC for left hippocampal volume is 0.92 with a 95% CI from 0.86 to 0.95, and the rank-based CCC for right hippocampal volume is 0.91 with a 95% CI from 0.86 to 0.95; both indicating excellent rank-based reproducibility of measuring hippocampal volumes. These findings are within the reported test-retest reliability range for repeat MRI visits on the same scanner (Han et al., 2006).

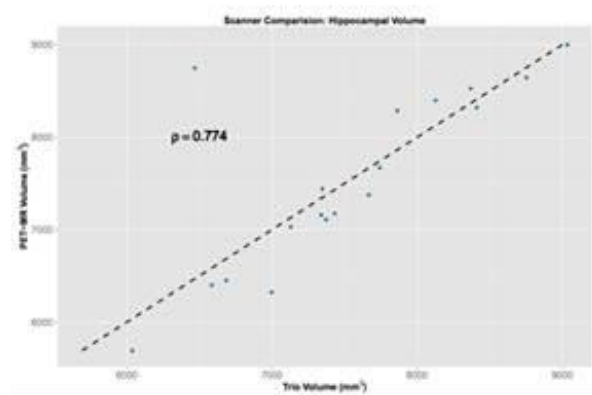


Figure 3. Hippocampal volume comparison of FreeSurfer derived hippocampal volumes from the Siemens TIM Trio 3T MRI and the Siemens Biograph mMR 3T PET-MR.

PET IMAGING

PET SCANNERS

Data included in OASIS was collected on the following scanners. Scanner specific information is recorded in dataset_description.json for each MR scan session. *For manuscripts, select only the scanner(s) from which your subset of data were derived.*

- Siemens Biograph mMR PET-MR 3T scanner (serial#: 51010)
- Siemens Biograph 40 PET/CT scanner (serial#: 1003)
- Siemens Biograph 128_Vision Edge PET/CT (serial#: 11009)
- Siemens ECAT HRplus 962 PET scanner (serial#: 101006)

HR+ IMAGE NOTES (PIB AND FDG)

ECAT PET images were acquired on either a Siemens 962 HR+ PET scanner. Emission data were reconstructed using a 3-D filter back-projection into a 128 x 128 x 63 matrix (2.12 x 2.12 x 2.43mm) with single scatter correction [1], a ramp filter (resolution of ~5.5-6 mm full-width half maximum [FWHM]), measured attenuation factors from a Ge-68 transmission scan, and randoms correction. These images have been converted from ECAT to NIFTI using dcm2niix (v1.0.20180404 GCC4.4.7).

All processed data have already been spatially smoothed to a FWHM of 8mm using the PET Unified Pipeline (PUP). To achieve a FWHM of 8mm for data harmonization of the ECAT images, we recommend the following Gaussian kernels to be in alignment with the Alzheimer's Disease Neuroimaging Initiative (ADNI) protocol FWHM all planes = 5.5 mm for the Siemens HR+.

TRACERS

PIB

N-methyl-[¹¹C]2-(4'-methylaminophenyl)-6-hydroxybenzothiazole ([¹¹C]PIB) is a radiolabeled compound that binds *in vivo* to brain amyloid deposits. Developed at the University of Pittsburgh, PIB has very high affinity for amyloid plaques. With administration of 6 - 20 mCi of [¹¹C]PIB, a 60 minute dynamic PET scan in 3D mode (septa retracted) will be initiated (24 x 5 sec frames; 9 x 20 sec frames; 10 x 1 min frames; 9 x 5 min frames).

AV45

Florbetapir binds to β -amyloid ($A\beta$) plaque utilizing the radioactive isotope ¹⁸F for use in PET scanning. Florbetapir F18 is used under the research number 18F-AV-45 and therefore referred to as AV45. Participants received a single i.v. administration of approximately 370 MBq (10 mCi) of florbetapir F 18 (over 10-60 sec). There are two acceptable procedures for obtaining the florbetapir F 18 PET scans:

1. In the preferred approach, the participant will be positioned in the PET-MR scanner at the time of injection and a 70-minute dynamic scan (with simultaneous PET and full Standard MR acquisition) will be

obtained starting at the time of injection. For florbetapir F 18 scans conducted on the PET/MR scanner, a short (approximately 15 minute) CT scan may be conducted on the PET/CT scanner.

2. For those participants who cannot tolerate the full exam, an alternative is to rest quietly in an uptake room for the first 40 minutes after injection. The participant will then be positioned in the PET-MR scanner to undergo a scan lasting 20 minutes, beginning 50 minutes after florbetapir F 18 injection and lasting for 20 minutes, using the Short MR Protocol. For florbetapir F 18 scans conducted on the PET/MR scanner, a short (approximately 15 minute) CT scan may be conducted on the PET/CT scanner.

FDG

Metabolic imaging with [18F]FDG-PET was performed with a 3D dynamic acquisition began 40 minutes after a bolus injection of approximately 5 mCi of FDG and lasted for 20 minutes.

AV1451

Flortaucipir binds to the paired helical filaments characteristic of neurofibrillary tau tangles in Alzheimer disease. Flortaucipir F18 is used under the research name 18F-AV-1451 and therefore referred to as AV1451. Participants received a single i.v. administration of approximately 370 MBq (10 mCi) of flortaucipir F18 (over 10-60 sec). There are three acceptable procedures for obtaining flortaucipir F18 PET scans:

1. In the preferred approach, the participant will be positioned in the PET/CT scanner at time of injection and a 105-minute dynamic scan will be acquired starting at time of injection.
2. For participants who cannot tolerate the full exam, an alternative is to rest quietly in an uptake room for the first 75-minutes after injection. The participant will then be positioned in the PET/CT to undergo a scan lasting 30 minutes.
3. A final alternative is a hybrid approach. In this method, the participant will be positioned in the PET/CT scanner at time of injection and a 60-minute dynamic scan will be acquired starting at time of injection. The participant will then have a 15-minute rest period where they are free to leave the scanner. Following this 15-minute break period, the participant will be placed back into the PET/CT and a 30-minute static scan will be acquired starting at 75-minutes post-injection. The two scans will be reconstructed separately from one another. This method accommodates participants who are unable to complete the full, uninterrupted exam while persevering early frame dynamic information.

POST-PROCESSED PET: PET UNIFIED PIPELINE (PUP)

PET imaging analyses are performed using the PET unified pipeline (PUP, <https://github.com/ysu001/PUP>) (Su 2013, Su 2015).

PET images are smoothed to achieve a common spatial resolution of 8mm to minimize inter-scanner differences (Joshi et al., 2009). Inter-frame motion correction for the dynamic PET images is performed using standard image registration techniques (Hajnal et al., 1995; Eisenstein et al., 2012). PET-MR registration is performed using a vector-gradient algorithm (VGM; Rowland et al., 2005) in a symmetric fashion (i.e. average transformation for PET-

>MR and inverse of MR->PET was used as the final transformation matrix). By default, regional PET processing is performed based on FreeSurfer segmentation (using wmparc.mgz as the region definition), and each FreeSurfer region is analyzed. The PET processing pipeline generates both reports of regional measurements as well as an SUVR image in the individual FreeSurfer space.

PUP VARIABLE NOMENCLATURE

Our data naming convention provides a standard for listing the region and the processing method (Table 8). Left and right brain structures use L and R. When left and right are averaged together the suffix includes the designation TOT. For a full list of variables see [PUP Variables](#). Six prefixes are used:

Table 9 PUP Nomenclature

Data Type	Definition	Example Name
fBP_	<i>FreeSurfer calculated Binding Potential</i>	fBP_TOT_ACCUMBENS
fBP_rsf_	<i>FreeSurfer calculated, partial volume corrected Binding Potential</i>	fBP_rsf_TOT_ACCUMBENS
fSUVR_	<i>FreeSurfer calculated SUVR</i>	fSUVR_TOT_ACCUMBENS
fSUVR_rsf_	<i>FreeSurfer calculated, partial volume corrected SUVR, the gold standard</i>	fSUVR_rsf_TOT_ACCUMBENS
ASL_	<i>Arterial Spin Labeled Cerebral Blood Flow</i>	ASL_TOT_ACCUMBENS
ASL_pvc_	<i>Arterial Spin Labeled Cerebral Blood Flow with Partial Volume Correction</i>	ASL_pvc_TOT_ACCUMBENS

Table 10 PUP prefixes (tracer+processed_outcome) examples

Tracer	Definition	Example Name
FDG	[18F]-Fluodeoxyglucose	FDG_fSUVR_TOT_ACCUMBENS
PiB	[11C]-Pittsburg Compound B	PiB_fBP_TOT_ACCUMBENS
AV45	[18F]-Florbetapir	AV45_fSUVR_TOT_ACCUMBENS

The prefixes (tracer+processed_outcome) are applied to the SAS correlate suffix to create a descriptive SAS compliant name (Table 9).

- PiB_fSUVR_rsf_TOT_CTX_PRECUNEUS is the [11C] PiB partial volume corrected SUVR of the gray matter in both the right and left FreeSurfer precuneus.
- FDG_fSUVR_rsf_TOT_WM_PRECUNEUS is the [18F] FDG partial volume corrected SUVR of the white matter calculated using the average activity in both the right and left FreeSurfer precuneus.
- FDG_fBP_TOT_CORTMEAN is the [18F] FDG average BP of the four MCBP cortical structures using FreeSurfer regions (TOTFS_PREFRN, TOTFS_TMP, TOTFS_GYREC, TOT_CTX_PRECUNEUS).

PARTIAL VOLUME CORRECTION

As PET images have low spatial resolution, measured signals are distorted by partial volume effects (PVE). The distortion caused by PVE is a function of the size and shape of the region of interest in addition to spatial resolution of the images. In longitudinal studies, the impact of PVE is further confounded by brain atrophy due to aging and pathological changes. To account for these distortions, correction technique is implemented in our processing pipeline using a regional spread function (RSF; Rousset 1998) based approach (Su 2015). We have demonstrated that the RSF technique was able to improve PET quantification and achieve better sensitivity to

longitudinal changes in amyloid burden (Su 2015, 2016). Our standard PET processing includes results both with and without RSF partial volume correction. Also, SUVR images are only available without partial volume correction in current analysis.

ALTERNATIVE REFERENCE REGION

As previously described, cerebellum cortex is used as the standard reference region for image quantification. However, for SUVR measurements, it is possible to renormalize to any alternative reference region by dividing the standard SUVR value by the SUVR value of the alternative reference region of choice:

$$\text{SUVR}_{\text{new}} = \text{SUVR}_{\text{std}} / \text{SUVR}_{\text{altref}}$$

AMYLOID PET IMAGING ANALYSIS

Currently, two amyloid imaging tracers are used in our studies, i.e. [11C]-Pittsburgh Compound B (PiB) and [18F]-Florbetapir (AV45). For both tracers, two modeling approaches are implemented: 1) binding potential (BP_{ND}) is calculated using Logan graphical analysis (Logan 1996; Mintun 2006; Su 2013, 2015, 2016), when full dynamic PET imaging data are available, i.e. PET acquisition was started in synchronization with tracer administration and PET images were reconstructed into multiple time frames; 2) regional target-to-reference intensity ratio, a.k.a, standard uptake ratio (SUVR), is estimated for all processable PET data.

Under standard protocol, quantitative PET analysis (both BP_{ND} and SUVR) uses 30 to 60 minutes post-injection as the time window for PiB, and 50 to 70 minutes for AV45; and the cerebellum cortex is used as the default reference region. To assess global amyloid burden based on amyloid PET imaging data, the arithmetic mean of BP_{ND} or SUVRs from precuneus (PREC), prefrontal cortex (PREF), gyrus rectus (GR), and lateral temporal (TEMP) regions are defined as the mean cortical binding potential (MCBP) or mean cortical SUVR (MCSUVR). In FreeSurfer based processing, PREC is defined as the combined left and right hemisphere ctx-precuneus, PREF is defined as the left and right combined ctx-superiorfrontal and ctx-rostralmiddlefrontal regions, GR is defined as the left and right combined ctx-lateralorbitofrontal and ctx-medialorbitofrontal regions, and TEMP is defined as the left and right combined ctx-superialtemporal and ctx-middletemporal regions (Fig. 4; Su 2013).

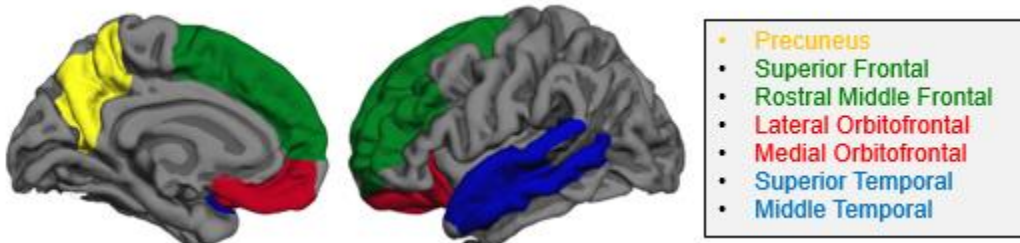


Figure 4 FreeSurfer regions for global amyloid burden index (MCBP, MCSUVR, etc) calculation.

CUTOFF VALUES FOR AMYLOID POSITIVITY

Traditionally, the cutoff for amyloid positivity has been established as MCBP>0.18 based on manually processed PiB data (Mintun 2006). We also established that the same cutoff could be used for FreeSurfer processing generated MCBP based on a study population of 77 participants (Su 2013). Based on this dataset, the cutoff for MCSUVRRSF was determined to be 1.42, the cutoff values for additional versions of global amyloid burden measurements that would generate best matched amyloid positivity classification as using manual MCBP=0.18 are also determined. For AV45, the equivalent cutoff to PiB MCSUVRRSF>1.42 was determined based on a sporadic AD cohort of 103 participants who had AV45-PiB crossover data based on the regression line between AV45 MCSUVRs and PiB MCSUVRRSF (Fig. 5) (Su 2019). The amyloid positivity cutoff using the cerebellar cortex reference region (Table 11), brainstem reference region (Table 12), and centiloid values (Table 13) are found below.

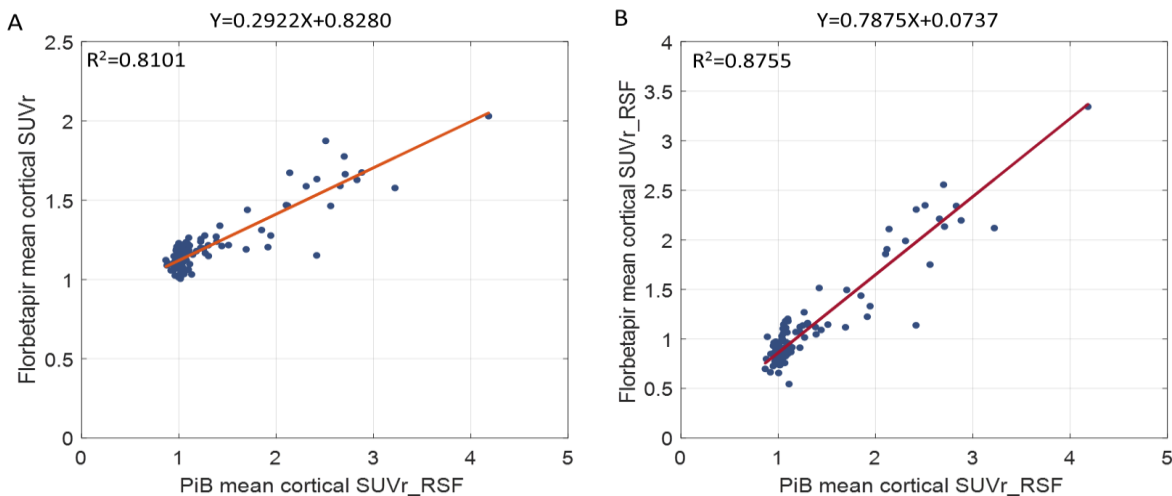


Figure 5. PiB-AV45 crossover dataset illustrating the relationship between AV45 based mean cortical SUVR and PiB based mean cortical SUVrs.

Table 11. Amyloid Positivity Cutoffs - Cerebellar Cortex Reference Region (*see Su et al 2019)

Amyloid Positivity Cutoffs - Cerebellar Cortex Reference Region	
PIB MCBP	0.18
PIB MCBP RSF	0.37
PIB MCSUVR	1.31
PIB MCUSVR RSF	1.42
AV45 MCSUVR	1.24 *
AV45 MCSUVR RSF	1.19 *

Table 12. Amyloid Positivity Cutoffs – Brainstem Reference Region

Amyloid Positivity Cutoffs – Brainstem Reference Region	
PIB MCSUVR BS	0.79
PIB MCUSVR RSF BS	0.72

Table 13. The equivalent cutoffs in Centiloid units were also derived by applying the Centiloid conversion equations described below to the native measurement cutoffs.

Amyloid Positivity Cutoffs - Centiloid	
CL PIB MCBP	18.2
CL PIB MCUSVR RSF	16.4
CL AV45 MCSUVR	21.9
CL AV45 MCSUVR RSF	20.6

CENTILOID CONVERSION FOR AMYLOID PET

Differences in the amyloid imaging tracer, the PET acquisition, and the analysis protocol across different studies introduce considerable variability within amyloid PET imaging data. This variability leads to difficulties in comparing and interpreting amyloid burden results reported from different groups (Klunk et al, 2015). To achieve comparable results, the Centiloid Working Group established a standardized scale called Centiloid to convert mean cortical SUVR and BP into a Centiloid measure of global amyloid disposition. If you want to use regional values, consult the Imaging Core.

The procedure and requirements to define the Centiloid scale is documented in detail in the initial Centiloid paper (Klunk et al 2015). To summarize, the Centiloid scale is defined by two anchor points: the mean amyloid burden measurement of a young control group with no amyloid pathology in their brain, represented as 0 in the Centiloid scale, and the mean amyloid burden of an AD group, represented as 100 in the Centiloid scale (level 1 calibration). Subsequently, a Deming regression and a linear transformation are performed to calibrate the tracer and the local processing methods to the Centiloid scale (i.e. level 2 calibration). Currently, both PiB and AV45 have been calibrated to the Centiloid scale for both non-partial volume and partial volume correction (rsf) using standard PUP (see equations below).

The PiB-Centiloid equations were defined using a subset of the Global Alzheimer's Association Information Network dataset (GAAIN, <http://www.gaain.org>) for PiB (30-60 minutes post-injection) SUVR and BP measures and were processed with cerebellar cortex, whole cerebellum, or brainstem as the reference region. Different reference regions have an impact on the mean Centiloid values and we suggest using the cerebellar cortex as the reference region since it has the least variability in the young control cohort (eq. 1 through 4). We found that our implementation of the standard Centiloid analysis is strongly correlated with the published Centiloid measures for the GAAIN data set ($r^2 = 0.99$).

The AV45-Centiloid equations (eq.5 and 6) were defined using a subset of the baseline DIAN trial unit (DIAN-TU) data set with PiB (40-70 minutes post-injection) and AV45 (50-70 minutes post-injection) imaging data for SUVR measures; the cerebellar cortex was used as the default reference region. A strong correlation ($r^2 = 0.79$) was found, shown in figure 6, between AV45 mean cortical SUVRs and PiB Centiloid SUVRs (SUVRs calculated through the Centiloid pipeline) (Klunk et al. 2015).

As any tracer or processing method can be scaled to Centiloid, new equations will be derived as new amyloid tracers and data become available. Centiloid equations may be recalibrated in the future to follow consensus of the research community.

Table 14. Centiloid conversion equations for PiB and AV45 using the "tot_cortmean" variable.

Centiloid Equations (TOT_CORTMEAN)	
$\text{PiB}_{\text{Centiloid}}_{\text{BP}} = 126.7 \times \text{PiB_3060_BP} - 4.4$	Eq.1
$\text{PiB}_{\text{Centiloid}}_{\text{SUVR}} = 111.8 \times \text{PiB_3060_SUVR} - 119.3$	Eq.2
$\text{PiB}_{\text{Centiloid}}_{\text{BPRSF}} = 53.9 \times \text{PiB_3060_BP_RSF} - 4.7$	Eq.3
$\text{PiB}_{\text{Centiloid}}_{\text{SUVRRSF}} = 45.0 \times \text{PiB_3060_SUVR_RSF} - 47.5$	Eq.4
$\text{AV45}_{\text{Centiloid}}_{\text{SUVR}} = 163.6 \times \text{AV45_SUVR} - 181.0$	Eq.5
$\text{AV45}_{\text{Centiloid}}_{\text{SUVRRSF}} = 53.6 \times \text{AV45_SUVR_RSF} - 43.2$	Eq.6

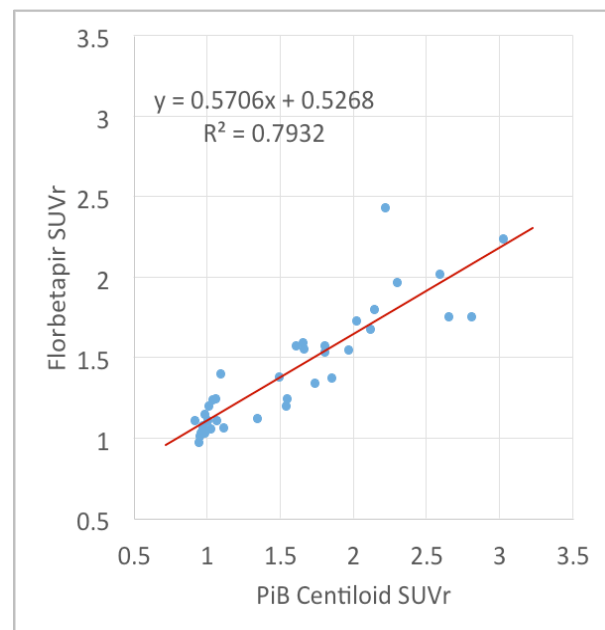


Figure 6 Comparison between PiB Centiloid SUVR and AV45 mean cortical SUVR for the DIAN-TU calibration dataset.

Table 15 below shows some examples on the conversion of non-partial volume corrected SUVR and BP to their respective Centiloid value.

Centiloid Value	PiB 30-60 min BP	PiB 30-60 min SUVR
-10	-0.0442	0.9776

0	0.0347	1.0671
25	0.2320	1.2907
50	0.4294	1.5143
75	0.6267	1.7379
100	0.8240	1.9615
110	0.9029	2.0510

ADRC conversion equations additionally have been defined between PiB (30-60 minutes post-injection) and AV45 (50-70 minutes post-injection) using the same DIAN-TU Centiloid calibration cohort (mentioned above) for the non-partial volume and partial volume corrected MCSUVRs measures (eq. 7 through 10).

Table 16 Conversion Equations between PiB and AV45 (TOT_CORTMEAN).

Conversion Equations between PiB and AV45 (TOT_CORTMEAN)	
PIB MCSUVR = $(AV45_MCSUVR - 0.3678) / 0.6942$	Eq.7
AV45 MCSUVR = $(PiB_3060_MCSUVR * 0.6942) + 0.3678$	Eq.8
PIB MCSUVRRSF = $(AV45_MCSUVR_RSF - 0.0238) / 0.7948$	Eq.9
AV45 MCSUVRRSF = $(PiB_3060_MCSUVR_RSF * 0.7948) + 0.0238$	Eq.10

TAU PET IMAGING (OASIS3_AV1451)

[¹⁸F]-Flortaucipir (AV-1451) previously known as T807 (Chien 2013) is currently used for in vivo imaging of tau pathology in Knight ADRC studies. Standard procedure for tau PET processing is identical to amyloid PET processing with the exception of the time window (80-100 minutes) that used for quantification.

Tau PET data is accessible in a separate protected project on central.xnat.org and linked to OASIS-3 subjects. Access can be granted by emailing the following information to oasis-brains@nrg.wustl.edu:

- 1 page summary of research proposal
- List of investigators to add (names and emails)
- Signed data use agreement (digital signature accepted)

BRAAK STAGING

The progression of Alzheimer disease related neurofibrillary pathology can be determined by Braak staging (Braak and Braak 1995). The six stages are calculated for the AV1451 tracer and included in the OASIS3_AV1451 sub-project releases (Table 17).

Table 17. The regions included in each Braak staging measure.

Braak Stage	FS Region Processing Name	Biostatistics Standardizations
1-2	ctx-entorhinal	fSUVR_rsf_TOT_CTX_ENTORHINAL
3-4	Amygdala	fSUVR_rsf_TOT_AMYGDALA
3-4	Accumbens-area	fSUVR_rsf_TOT_ACCUMBENS
3-4	hippocampus	fSUVR_rsf_TOT_HIPPOCAMPUS
3-4	ctx-insula	fSUVR_rsf_TOT_CTX_INSULA
3-4	ctx-medialorbitofrontal	fSUVR_rsf_TOT_CTX_MEDORBFRN
3-4	ctx-lateralorbitofrontal	fSUVR_rsf_TOT_CTX_LATORBFRN
3-4	ctx-parorbitalis	fSUVR_rsf_TOT_CTX_PARSORBLIS
3-4	ctx-parahippocampal	fSUVR_rsf_TOT_CTX_PARAHPCMPL
3-4	ctx-rostralanteriorcingulate	fSUVR_rsf_TOT_CTX_ROSANTCNG
3-4	ctx-posteriorcingulate	fSUVR_rsf_TOT_CTX_POSTCNG
3-4	ctx-caudalanteriorcingulate	fSUVR_rsf_TOT_CTX_CAUDANTCNG
3-4	ctx-isthmuscingulate	fSUVR_rsf_TOT_CTX_ISTHMUSCNG
5-6	ctx-bankssts	fSUVR_rsf_TOT_CTX_SSTS BANK
5-6	ctx-middletemporal	fSUVR_rsf_TOT_CTX_MIDTMP
5-6	ctx-caudalmiddlefrontal	fSUVR_rsf_TOT_CTX_CAUDMIDFRN
5-6	ctx-fusiform	fSUVR_rsf_TOT_CTX_FUSIFORM
5-6	ctx-inferiorparietal	fSUVR_rsf_TOT_CTX_INFERPRTL
5-6	ctx-inferiortemporal	fSUVR_rsf_TOT_CTX_INFERTMP
5-6	ctx-lateraloccipital	fSUVR_rsf_TOT_CTX_LATOCC
5-6	ctx-supramarginal	fSUVR_rsf_TOT_CTX_SUPRAMRGNL
5-6	ctx-precuneus	fSUVR_rsf_TOT_CTX_PRECUNEUS

CUTOFF VALUES FOR TAU POSITIVITY

A tau summary measure, labeled as ‘tauopathy’, has been defined by our group to be the arithmetic mean of the partial volume corrected SUVRs from the amygdala, entorhinal cortex, inferior temporal region, and lateral occipital cortex defined using Freesurfer. (Mishra et al., 2017). Tables 18 specifies the tau positivity cutoff using the tauopathy measure.

Table 18. Tau positivity cutoff - Cerebellar Cortex Reference Region

Tau Positivity Cutoff - Cerebellar Cortex Reference Region	
AV-1451 Tauopathy	1.22

FREESURFER VARIABLES

Below is a list of the Freesurfer variables as found in OASIS-3 and a suggested list of SAS compatible labels.

MRI Freesurfer Default Variable	SAS Compatible Variable Labels
3rd-Ventricle	MR_TOTV_THIRDVENT
4th-Ventricle	MR_TOTV_FOURTHVENT
5th-Ventricle	MR_TOTV_FIFTHVENT
Brain-Stem	MR_TOTV_BRAINSTEM
CC_Anterior	MR_TOTV_CRPCLM_ANT
CC_Central	MR_TOTV_CRPCLM_CNTRL
CC_Mid_Anterior	MR_TOTV_CRPCLM_MID_ANT
CC_Mid_Posterior	MR_TOTV_CRPCLM_MID_POST
CC_Posterior	MR_TOTV_CRPCLM_POST
CortexVol	MR_TOTV_CORTEX
CSF	MR_TOTV_CSF
IntraCranialVol	MR_TOTV_INTRACRANIAL
non-WM-hypointensities	MR_TOTV_NONWMHPOINTENSITIES
Optic-Chiasm	MR_TOTV_OPTICHIASM
SubCortGrayVol	MR_TOTV_SUBCORTGRAY
TotalGrayVol	MR_TOTV_GRAY
WM-hypointensities	MR_TOTV_WMHPOINTENSITIES
lh_bankssts_thickness	MR_LT_SSSTSBANK
lh_caudalanteriorcingulate_thickness	MR_LT_CAUDANTCNG
lh_caудалmiddlefrontal_thickness	MR_LT_CAUDMIDFRN
lh_cuneus_thickness	MR_LT_CUNEUS
lh_entorhinal_thickness	MR_LT_ENTORHINAL
lh_frontalpole_thickness	MR_LT_FRNPOL
lh_fusiform_thickness	MR_LT_FUSIFORM
lh_inferiorparietal_thickness	MR_LT_INFRPRTL
lh_inferiortemporal_thickness	MR_LT_INFRTMP
lh_insula_thickness	MR_LT_INSULA
lh_isthmuscingulate_thickness	MR_LT_ISTMUSCNG
lh_lateraloccipital_thickness	MR_LT_LATOCC
lh_lateralorbitofrontal_thickness	MR_LT_LATORBFRN
lh_lingual_thickness	MR_LT_LINGUAL
lh_medialorbitofrontal_thickness	MR_LT_MEDORBFRN
lh_middletemporal_thickness	MR_LT_MIDTMP
lh_paracentral_thickness	MR_LT_PARACNTRL
lh_parahippocampal_thickness	MR_LT_PARAHPCMPL
lh_parsopercularis_thickness	MR_LT_PARAOPRCLRS
lh_parsorbitalis_thickness	MR_LT_PARSORBL
lh_parstriangularis_thickness	MR_LT_PARSTRNGLRS
lh_pericalcarine_thickness	MR_LT_PERICLCRN
lh_postcentral_thickness	MR_LT_POSTCNTRL
lh_posteriorcingulate_thickness	MR_LT_POSTCNG
lh_precentral_thickness	MR_LT_PRECNTRL
lh_precuneus_thickness	MR_LT_PRECUNEUS
lh_rostralanteriorcingulate_thickness	MR_LT_ROSANTCNG
lh_rostralmiddlefrontal_thickness	MR_LT_ROSMIDFRN
lh_superiorfrontal_thickness	MR_LT_SUPERFRN
lh_superiorparietal_thickness	MR_LT_SUPERRRTL
lh_superiortemporal_thickness	MR_LT_SUPERTMP
lh_supramarginal_thickness	MR_LT_SUPRAMRGNL
lh_temporalpole_thickness	MR_LT_TMPPOLE
lh_transversetemporal_thickness	MR_LT_TRANSTMP
rh_bankssts_thickness	MR_RT_SSSTSBANK
rh_caudalanteriorcingulate_thickness	MR_RT_CAUDANTCNG
rh_caудалmiddlefrontal_thickness	MR_RT_CAUDMIDFRN

rh_cuneus_thickness	MR_RT_CUNEUS
rh_entorhinal_thickness	MR_RT_ENTORHINAL
rh_frontalpole_thickness	MR_RT_FRNPOLE
rh_fusiform_thickness	MR_RT_FUSIFORM
rh_inferiorparietal_thickness	MR_RT_INFRPRTL
rh_inferiortemporal_thickness	MR_RT_INFRTMP
rh_insula_thickness	MR_RT_INSULA
rh_isthmuscingulate_thickness	MR_RT_ISTMUSCNG
rh_lateraloccipital_thickness	MR_RT_LATOCC
rh_lateralorbitofrontal_thickness	MR_RT_LATORBFRN
rh_lingual_thickness	MR_RT_LINGUAL
rh_medialorbitofrontal_thickness	MR_RT_MEDORBFRN
rh_middletemporal_thickness	MR_RT_MIDTMP
rh_paracentral_thickness	MR_RT_PARACNTRL
rh_parahippocampal_thickness	MR_RT_PARAHPCMPL
rh_parsopercularis_thickness	MR_RT_PARAOPRCLRS
rh_parsorbitalis_thickness	MR_RT_PARSORBLS
rh_parstriangularis_thickness	MR_RT_PARSTRNGLRS
rh_pericalcarine_thickness	MR_RT_PERICLCRN
rh_postcentral_thickness	MR_RT_POSTCNTRL
rh_posteriorcingulate_thickness	MR_RT_POSTCNG
rh_precentral_thickness	MR_RT_PRECNTRL
rh_precuneus_thickness	MR_RT_PRECUNEUS
rh_rostralanteriorcingulate_thickness	MR_RT_ROSANTCNG
rh_rostralmiddlefrontal_thickness	MR_RT_ROSMIDFRN
rh_superiorfrontal_thickness	MR_RT_SUPERFRN
rh_superiorparietal_thickness	MR_RT_SUPERPRTL
rh_superiortemporal_thickness	MR_RT_SUPERTMP
rh_supramarginal_thickness	MR_RT_SUPRAMRGNL
rh_temporalpole_thickness	MR_RT_TMPPOLE
rh_transversetemporal_thickness	MR_RT_TRANSTMP
Left-Accumbens-area	MR_LV_ACCUMBENS
Left-Amygdala	MR_LV_AMYGDALA
Left-Caudate	MR_LV_CAUD
Left-Cerebellum-Cortex	MR_LV_CBLL_COREX
Left-Cerebellum-White-Matter	MR_LV_CBLL_WM
Left-choroid-plexus	MR_LV_CHORPLEX
Left-Hippocampus	MR_LV_HIPPOCAMPUS
Left-Inf-Lat-Vent	MR_LV_INFLATVENT
Left-Lateral-Ventrie	MR_LV_LATVENT
Left-non-WM-hypointensities	MR_LV_NONWMHYPOINTENSITIES
Left-Pallidum	MR_LV_PALLIDUM
Left-Putamen	MR_LV_PUTAMEN
Left-Thalamus-Proper	MR_LV_THALAMUS
Left-VentralDC	MR_LV_VENTRALDC
Left-vessel	MR_LV_VESSEL
Left-WM-hypointensities	MR_LV_WMHYPPOINTENSITIES
lh_bankssts_volume	MR_LV_SSTS BANK
lh_caudalanteriorcingulate_volume	MR_LV_CAUDANTCNG
lh_caudalmiddlefrontal_volume	MR_LV_CAUDMIDFRN
lh_cuneus_volume	MR_LV_CUNEUS
lh_entorhinal_volume	MR_LV_ENTORHINAL
lh_frontalpole_volume	MR_LV_FRNPOLE
lh_fusiform_volume	MR_LV_FUSIFORM
lh_inferiorparietal_volume	MR_LV_INFRPRTL
lh_inferiortemporal_volume	MR_LV_INFRTMP
lh_insula_volume	MR_LV_INSULA
lh_isthmuscingulate_volume	MR_LV_ISTMUSCNG
lh_lateraloccipital_volume	MR_LV_LATOCC
lh_lateralorbitofrontal_volume	MR_LV_LATORBFRN
lh_lingual_volume	MR_LV_LINGUAL
lh_medialorbitofrontal_volume	MR_LV_MEDORBFRN
lh_middletemporal_volume	MR_LV_MIDTMP

lh_paracentral_volume	MR_LV_PARACNTRL
lh_parahippocampal_volume	MR_LV_PARAHPCMPL
lh_parsopercularis_volume	MR_LV_PARAOPRCLRS
lh_parsorbitalis_volume	MR_LV_PARSORBLS
lh_parstriangularis_volume	MR_LV_PARSTRNGLRS
lh_pericalcarine_volume	MR_LV_PERICLCRN
lh_postcentral_volume	MR_LV_POSTCNTRL
lh_posteriorcingulate_volume	MR_LV_POSTCNG
lh_precentral_volume	MR_LV_PRECNTRL
lh_precuneus_volume	MR_LV_PRECUNEUS
lh_rostralanteriorcingulate_volume	MR_LV_ROSANTCNG
lh_rostralmiddlefrontal_volume	MR_LV_ROSMIDFRN
lh_superiorfrontal_volume	MR_LV_SUPERFRN
lh_superiorparietal_volume	MR_LV_SUPERPRTL
lh_superiortemporal_volume	MR_LV_SUPERTMP
lh_supramarginal_volume	MR_LV_SUPRAMRGNL
lh_temporalpole_volume	MR_LV_TMPPOLE
lh_transversetemporal_volume	MR_LV_TRANSTMP
lhCortexVol	MR_LV_Cortex
lhCorticalWhiteMatterVol	MR_LV_CORTICALWM
rh_bankssts_volume	MR_RV_SSSTSBANK
rh_caudalanteriorcingulate_volume	MR_RV_CAUDANTCNG
rh_caудалmiddlefrontal_volume	MR_RV_CAUDMIDFRN
rh_cuneus_volume	MR_RV_CUNEUS
rh_entorhinal_volume	MR_RV_ENTORHINAL
rh_frontalpole_volume	MR_RV_FRNPOLE
rh_fusiform_volume	MR_RV_FUSIFORM
rh_inferiorparietal_volume	MR_RV_INFRPRTL
rh_inferiortemporal_volume	MR_RV_INFRTMP
rh_insula_volume	MR_RV_INSULA
rh_isthmuscingulate_volume	MR_RV_ISTMUSCNG
rh_lateraloccipital_volume	MR_RV_LATOCC
rh_lateralorbitofrontal_volume	MR_RV_LATORBFRN
rh_lingual_volume	MR_RV_LINGUAL
rh_medialorbitofrontal_volume	MR_RV_MEDORBFRN
rh_middletemporal_volume	MR_RV_MIDTMP
rh_paracentral_volume	MR_RV_PARACNTRL
rh_parahippocampal_volume	MR_RV_PARAHPCMPL
rh_parsopercularis_volume	MR_RV_PARAOPRCLRS
rh_parsorbitalis_volume	MR_RV_PARSORBLS
rh_parstriangularis_volume	MR_RV_PARSTRNGLRS
rh_pericalcarine_volume	MR_RV_PERICLCRN
rh_postcentral_volume	MR_RV_POSTCNTRL
rh_posteriorcingulate_volume	MR_RV_POSTCNG
rh_precentral_volume	MR_RV_PRECNTRL
rh_precuneus_volume	MR_RV_PRECUNEUS
rh_rostralanteriorcingulate_volume	MR_RV_ROSANTCNG
rh_rostralmiddlefrontal_volume	MR_RV_ROSMIDFRN
rh_superiorfrontal_volume	MR_RV_SUPERFRN
rh_superiorparietal_volume	MR_RV_SUPERPRTL
rh_superiortemporal_volume	MR_RV_SUPERTMP
rh_supramarginal_volume	MR_RV_SUPRAMRGNL
rh_temporalpole_volume	MR_RV_TMPPOLE
rh_transversetemporal_volume	MR_RV_TRANSTMP
rhCortexVol	MR_RV_Cortex
rhCorticalWhiteMatterVol	MR_RV_CORTICALWM
Right-Accumbens-area	MR_RV_ACCUMBENS
Right-Amygdala	MR_RV_AMYGDALA
Right-Caudate	MR_RV_CAUD
Right-Cerebellum-Cortex	MR_RV_CBLL_COREX
Right-Cerebellum-White-Matter	MR_RV_CBLL_WM
Right-choroid-plexus	MR_RV_CHORPLEX
Right-Hippocampus	MR_RV_HIPPOCAMPUS

Right-Inf-Lat-Vent	MR_RV_INFVENT
Right-Lateral-Ventricle	MR_RV_LATVENT
Right-non-WM-hypointensities	MR_RV_NONWMHPOINTENSITIES
Right-Pallidum	MR_RV_PALLIDUM
Right-Putamen	MR_RV_PUTAMEN
Right-Thalamus-Proper	MR_RV_THALAMUS
Right-VentralDC	MR_RV_VENTRALDC
Right-vessel	MR_RV_VESSEL
Right-WM-hypointensities	MR_RV_WMHPOINTENSITIES

PUP VARIABLES

Below is a list of the Pet Unified Pipeline (PUP) variables as found in OASIS-3 and a suggested list of SAS compatible labels. The prefixes (tracer+processed_outcome) are applied to the SAS correlate suffix to create a descriptive SAS compliant name (ex: PiB_mSUVR_TOT_ACCUMBENS).

Structure Name	SAS Compatible Variable Labels
Accumbens_area	TOT_ACCUMBENS
Amygdala	TOT_AMYGDALA
Brain_Stem	TOT_BRAINSTEM
Caudate	TOT_CAUD
CC_Anterior	CRPCLM_ANT
CC_Central	CRPCLM_CNTRL
CC_Mid_Anterior	CRPCLM_MID_ANT
CC_Mid_Posterior	CRPCLM_MID_POST
CC_Posterior	CRPCLM_POST
Cerebellum_Cortex	TOT_CBLL_CORTEX
Cerebellum_White_Matter	TOT_CBLL_WM
choroid_plexus	TOT_CHORPLEX
ctx_bankssts	TOT_CTX_SSTS BANK
ctx_caudalanteriorcingulate	TOT_CTX_CAUDANTCNG
ctx_caudalmiddlefrontal	TOT_CTX_CAUDMIDFRN
ctx_corpuscallosum	TOT_CTX_CRPCLM
ctx_cuneus	TOT_CTX_CUNEUS
ctx_entorhinal	TOT_CTX_ENTORHINAL
ctx_frontalpole	TOT_CTX_FRNPOLE
ctx_fusiform	TOT_CTX_FUSIFORM
ctx_inferiorparietal	TOT_CTX_INFERPRTL
ctx_inferiotemporal	TOT_CTX_INFERTMP
ctx_insula	TOT_CTX_INSULA
ctx_isthmuscingulate	TOT_CTX_ISTHMUSCNG
ctx_lateraloccipital	TOT_CTX_LATOCC
ctx_lateralorbitofrontal	TOT_CTX_LATORBFRN
ctx_lh_bankssts	L_CTX_SSTS BANK
ctx_lh_caudalanteriorcingulate	L_CTX_CAUDANTCNG
ctx_lh_caudalmiddlefrontal	L_CTX_CAUDMIDFRN
ctx_lh_corpuscallosum	L_CTX_CRPCLM
ctx_lh_cuneus	L_CTX_CUNEUS
ctx_lh_entorhinal	L_CTX_ENTORHINAL
ctx_lh_frontalpole	L_CTX_FRNPOLE
ctx_lh_fusiform	L_CTX_FUSIFORM
ctx_lh_inferiorparietal	L_CTX_INFRPRTL
ctx_lh_inferiotemporal	L_CTX_INFRTMP
ctx_lh_insula	L_CTX_INSULA
ctx_lh_isthmuscingulate	L_CTX_ISTHMUSCNG
ctx_lh_lateraloccipital	L_CTX_LATOCC
ctx_lh_lateralorbitofrontal	L_CTX_LATORBFRN
ctx_lh_lingual	L_CTX_LINGUAL
ctx_lh_medialorbitofrontal	L_CTX_MEDORBFRN
ctx_lh_middletemporal	L_CTX_MIDTMP

ctx_lh_paracentral	L_CTX_PARACNTRL
ctx_lh_parahippocampal	L_CTX_PARAHPCMPL
ctx_lh_parsopercularis	L_CTX_PARSOPRCLRS
ctx_lh_parsorbitalis	L_CTX_PARSORBLS
ctx_lh_parstriangularis	L_CTX_PARSTRNGLRS
ctx_lh_pericalcarine	L_CTX_PERICLCRN
ctx_lh_postcentral	L_CTX_POSTCNTRL
ctx_lh_posteriorcingulate	L_CTX_POSTCNG
ctx_lh_precentral	L_CTX_PRECNTRL
ctx_lh_precuneus	L_CTX_PRECUNEUS
ctx_lh_rostralanteriorcingulate	L_CTX_ROSANTCNG
ctx_lh_rostralmiddlefrontal	L_CTX_ROSMIDFRN
ctx_lh_superiorfrontal	L_CTX_SUPERFRN
ctx_lh_superioparietal	L_CTX_SUPERPRTL
ctx_lh_superiortemporal	L_CTX_SUPERTMP
ctx_lh_supramarginal	L_CTX_SUPRAMRGNL
ctx_lh_temporalpole	L_CTX_TMPPOLE
ctx_lh_transversetemporal	L_CTX_TRANSTMP
ctx_lingual	TOT_CTX_LINGUAL
ctx_medialorbitofrontal	TOT_CTX_MEDORBFRN
ctx_middletemporal	TOT_CTX_MIDTMP
ctx_paracentral	TOT_CTX_PARACNTRL
ctx_parahippocampal	TOT_CTX_PARAHPCMPL
ctx_parsopercularis	TOT_CTX_PARSOPRCLRS
ctx_parsorbitalis	TOT_CTX_PARSORBLS
ctx_parstriangularis	TOT_CTX_PARSTRNGLRS
ctx_pericalcarine	TOT_CTX_PERICLCRN
ctx_postcentral	TOT_CTX_POSTCNTRL
ctx_posteriorcingulate	TOT_CTX_POSTCNG
ctx_precentral	TOT_CTX_PRECNTRL
ctx_precuneus	TOT_CTX_PRECUNEUS
ctx_rh_bankssts	R_CTX_SSTS BANK
ctx_rh_caudalanteriorcingulate	R_CTX_CAUDANTCNG
ctx_rh_caudalmiddlefrontal	R_CTX_CAUDMIDFRN
ctx_rh_corpuscallosum	R_CTX_CRPCLM
ctx_rh_cuneus	R_CTX_CUNEUS
ctx_rh_entorhinal	R_CTX_ENTORHINAL
ctx_rh_frontalpole	R_CTX_FRNPOLE
ctx_rh_fusiform	R_CTX_FUSIFORM
ctx_rh_inferiorparietal	R_CTX_INFPRTL
ctx_rh_inferiortemporal	R_CTX_INF TMP
ctx_rh_insula	R_CTX_INSULA
ctx_rh_isthmuscingulate	R_CTX_ISTHMUSCNG
ctx_rh_lateraloccipital	R_CTX_LATOCC
ctx_rh_lateralorbitofrontal	R_CTX_LATORBFRN
ctx_rh_lingual	R_CTX_LINGUAL
ctx_rh_medialorbitofrontal	R_CTX_MEDORBFRN
ctx_rh_middletemporal	R_CTX_MIDTMP
ctx_rh_paracentral	R_CTX_PARACNTRL
ctx_rh_parahippocampal	R_CTX_PARAHPCMPL
ctx_rh_parsopercularis	R_CTX_PARSOPRCLRS
ctx_rh_parsorbitalis	R_CTX_PARSORBLS
ctx_rh_parstriangularis	R_CTX_PARSTRNGLRS
ctx_rh_pericalcarine	R_CTX_PERICLCRN
ctx_rh_postcentral	R_CTX_POSTCNTRL
ctx_rh_posteriorcingulate	R_CTX_POSTCNG
ctx_rh_precentral	R_CTX_PRECNTRL
ctx_rh_precuneus	R_CTX_PRECUNEUS
ctx_rh_rostralanteriorcingulate	R_CTX_ROSANTCNG
ctx_rh_rostralmiddlefrontal	R_CTX_ROSMIDFRN
ctx_rh_superiorfrontal	R_CTX_SUPERFRN
ctx_rh_superioparietal	R_CTX_SUPERPRTL
ctx_rh_superiortemporal	R_CTX_SUPERTMP

ctx_rh_supramarginal	R_CTX_SUPRAMRGNL
ctx_rh_temporalpole	R_CTX_TMPPOLE
ctx_rh_transversetemporal	R_CTX_TRANSTMP
ctx_rostralanteriorcingulate	TOT_CTX_ROSANTCNG
ctx_rostralmiddlefrontal	TOT_CTX_ROSMIDFRN
ctx_superiorfrontal	TOT_CTX_SUPERFRN
ctx_superiorparietal	TOT_CTX_SUPERPRTL
ctx_superiortemporal	TOT_CTX_SUPERTMP
ctx_supramarginal	TOT_CTX_SUPRAMRGNL
ctx_temporalpole	TOT_CTX_TMPPOLE
ctx_transversetemporal	TOT_CTX_TRANSTMP
GR_FS	TOTFS_GYREC
Hippocampus	TOT_HIPPOCAMPUS
Left_Accumbens_area	L_ACCUMBENS
Left_Amygdala	L_AMYGDALA
Left_Caudate	L_CAUD
Left_Cerebellum_Cortex	L_CTX_CBLL
Left_Cerebellum_White_Matter	L_WM_CBLL
Left_choroid_plexus	L_CHORPLEX
Left_Hippocampus	L_HIPPOCAMPUS
Left_Pallidum	L_PALLIDUM
Left_Putamen	L_PUTAMEN
Left_Substancia_Nigra	L_SUBSTNCA_NGRA
Left_Thalamus_Proper	L_THALAMUS
Left_UnsegmentedWhiteMatter	L_WM_UNSEGMENTED
Left_VentralDC	L_VENTRALDC
OCC_FS	TOTFS_OCC
Pallidum	TOT_PALLIDUM
PREF_FS	TOTFS_PREFRN
Putamen	TOT_PUTAMEN
Right_Accumbens_area	R_ACCUMBENS
Right_Amygdala	R_AMYGDALA
Right_Caudate	R_CAUD
Right_Cerebellum_Cortex	R_CTX_CBLL
Right_Cerebellum_White_Matter	R_WM_CBLL
Right_choroid_plexus	R_CHORPLEX
Right_Hippocampus	R_HIPPOCAMPUS
Right_Pallidum	R_PALLIDUM
Right_Putamen	R_PUTAMEN
Right_Substancia_Nigra	R_SUBSTNCA_NGRA
Right_Thalamus_Proper	R_THALAMUS
Right_UnsegmentedWhiteMatter	R_WM_UNSEGMENTED
Right_VentralDC	R_VENTRALDC
Substancia_Nigra	TOT_SUBSTNCA_NGRA
TEMP_FS	TOTFS_TMP
Thalamus_Proper	TOT_THALAMUS_PRPR
UnsegmentedWhiteMatter	TOT_WM_UNSEGMENTED
VentralDC	TOT_VENTRALDC
wm_bankssts	TOT_WM_SSTSBNK
wm_caudalanteriorcingulate	TOT_WM_CAUDANTCNG
wm_caudalmiddlefrontal	TOT_WM_CAUDMIDFRN
wm_corpuscallosum	TOT_WM_CRPCLM
wm_cuneus	TOT_WM_CUNEUS
wm_entorhinal	TOT_WM_ENTORHINAL
wm_frontalpole	TOT_WM_FRNPOLE
wm_fusiform	TOT_WM_FUSIFORM
wm_inferiorparietal	TOT_WM_INFERPRTL
wm_inferiortemporal	TOT_WM_INFERTMP
wm_insula	TOT_WM_INSULA
wm_isthmuscingulate	TOT_WM_ISTMUSCNG
wm_lateraloccipital	TOT_WM_LATOCC
wm_lateralorbitofrontal	TOT_WM_LATORBFRN
wm_lh_bankssts	L_WM_SSTSBNK

wm_lh_caudalanteriorcingulate	L_WM_CAUDANTCNG
wm_lh_caudalmiddlefrontal	L_WM_CAUDMIDFRN
wm_lh_corpuscallosum	L_WM_CRPCLM
wm_lh_cuneus	L_WM_CUNEUS
wm_lh_entorhinal	L_WM_ENTORHINAL
wm_lh_frontalpole	L_WM_FRNPOLE
wm_lh_fusiform	L_WM_FUSIFORM
wm_lh_inferiorparietal	L_WM_INFPRRTL
wm_lh_inferiortemporal	L_WM_INFTRMP
wm_lh_insula	L_WM_INSULA
wm_lh_isthmuscingulate	L_WM_ISTHMUSCNG
wm_lh_lateraloccipital	L_WM_LATOCC
wm_lh_lateralorbitofrontal	L_WM_LATORBFRN
wm_lh_lingual	L_WM_LINGUAL
wm_lh_medialorbitofrontal	L_WM_MEDORBFRN
wm_lh_middletemporal	L_WM_MIDTMP
wm_lh_paracentral	L_WM_PARACNTRL
wm_lh_parahippocampal	L_WM_PARAHPCMPL
wm_lh_parsopercularis	L_WM_PARSOPLRS
wm_lh_parsorbitalis	L_WM_PARSORBL
wm_lh_parstriangularis	L_WM_PARSTRNGRLS
wm_lh_pericalcarine	L_WM_PERICLCRN
wm_lh_postcentral	L_WM_POSTCNTRL
wm_lh_posteriorcingulate	L_WM_POSTCNG
wm_lh_precentral	L_WM_PRECNTRL
wm_lh_precuneus	L_WM_PRECUNEUS
wm_lh_rostralanteriorcingulate	L_WM_ROSANTCNG
wm_lh_rostralmiddlefrontal	L_WM_ROSMIDFRN
wm_lh_superiorfrontal	L_WM_SUPERFRN
wm_lh_superiorparietal	L_WM_SUPERPRTL
wm_lh_superiortemporal	L_WM_SUPERTMP
wm_lh_supramarginal	L_WM_SUPRAMRGNL
wm_lh_temporalpole	L_WM_TMPPOLE
wm_lh_transversetemporal	L_WM_TRANSTMP
wm_lingual	TOT_WM_LINGUAL
wm_medialorbitofrontal	TOT_WM_MEDORBFRN
wm_middletemporal	TOT_WM_MIDTMP
wm_paracentral	TOT_WM_PARACNTRL
wm_parahippocampal	TOT_WM_PARAHPCMPL
wm_parsopercularis	TOT_WM_PARSOPLRS
wm_parsorbitalis	TOT_WM_PARSORBL
wm_parstriangularis	TOT_WM_PARSTRNGRLS
wm_pericalcarine	TOT_WM_PERICLCRN
wm_postcentral	TOT_WM_POSTCNTRL
wm_posteriorcingulate	TOT_WM_POSTCNG
wm_precentral	TOT_WM_PRECNTRL
wm_precuneus	TOT_WM_PRECUNEUS
wm_rh_bankssts	R_WM_SSTS BANK
wm_rh_caudalanteriorcingulate	R_WM_CAUDANTCNG
wm_rh_caudalmiddlefrontal	R_WM_CAUDMIDFRN
wm_rh_corpuscallosum	R_WM_CRPCLM
wm_rh_cuneus	R_WM_CUNEUS
wm_rh_entorhinal	R_WM_ENTORHINAL
wm_rh_frontalpole	R_WM_FRNPOLE
wm_rh_fusiform	R_WM_FUSIFORM
wm_rh_inferiorparietal	R_WM_INFERIORPRTL
wm_rh_inferiortemporal	R_WM_INFERIORTMP
wm_rh_insula	R_WM_INSULA
wm_rh_isthmuscingulate	R_WM_ISTHMUSCNG
wm_rh_lateraloccipital	R_WM_LATOCC
wm_rh_lateralorbitofrontal	R_WM_LATORBFRN
wm_rh_lingual	R_WM_LINGUAL
wm_rh_medialorbitofrontal	R_WM_MEDORBFRN

wm_rh_middletemporal	R_WM_MIDTMP
wm_rh_paracentral	R_WM_PARACNTRL
wm_rh_parahippocampal	R_WM_PARAHPCMPL
wm_rh_parsopercularis	R_WM_PARSOPIRCLRS
wm_rh_parsorbitalis	R_WM_PARSORBLS
wm_rh_parstriangularis	R_WM_PARSTRNGLRS
wm_rh_pericalcarine	R_WM_PERICLCRN
wm_rh_postcentral	R_WM_POSTCNTRL
wm_rh_posteriorcingulate	R_WM_POSTCNG
wm_rh_precentral	R_WM_PRECNTRL
wm_rh_precuneus	R_WM_PRECUNEUS
wm_rh_rostralanteriorcingulate	R_WM_ROSANTCNG
wm_rh_rostralmiddlefrontal	R_WM_ROSMIDFRN
wm_rh_superiorfrontal	R_WM_SUPERFRN
wm_rh_superiorparietal	R_WM_SUPERPRTL
wm_rh_superiortemporal	R_WM_SUPERTMP
wm_rh_supramarginal	R_WM_SUPRAMRGNL
wm_rh_temporalpole	R_WM_TMPPOLE
wm_rh_transversetemporal	R_WM_TRANSTMP
wm_rostralanteriorcingulate	TOT_WM_ROSANTCNG
wm_rostralmiddlefrontal	TOT_WM_ROSMIDFRN
wm_superiorfrontal	TOT_WM_SUPERFRN
wm_superiorparietal	TOT_WM_SUPERPRTL
wm_superiortemporal	TOT_WM_SUPERTMP
wm_supramarginal	TOT_WM_SUPRAMRGNL
wm_temporalpole	TOT_WM_TMPPOLE
wm_transversetemporal	TOT_WM_TRANSTMP
MCBP	TOT_CORTMEAN

REFERENCES

1. Gorgolewski, K.J., et al. The brain imaging data structure, a format for organizing and describing outputs of neuroimaging experiments. *Sci Data* 2016; 3:160044. PMID: 27326542 PMCID: PMC4978148 DOI: 10.1038/sdata.2016.44.
2. Chien DT, Bahri S, Szardenings AK, Walsh JC, Mu F, Su M-Y, et al. Early Clinical PET Imaging Results with the Novel PHF-Tau Radioligand [F-18]-T807. *J. Alzheimer's Dis.* 2013; 34: 457–468.
3. Eisenstein, S.A., Koller, J.M., Piccirillo, M., Kim, A., Antenor-Dorsey, J.A., Videen, T.O., Snyder, A.Z., Karimi, M., Moerlein, S.M., Black, K.J., Perlmuter, J.S., Hershey, T., 2012. Characterization of extrastriatal D2 in vivo specific binding of [(1)(8)F](N-methyl)benperidol using PET. *Synapse* 66, 770-780.
4. Fischl B. FreeSurfer. *NeuroImage* 2012; 62(2):774-781. PMCID: PMC: 222857
5. Frouin V, Comtat C, Reilhac A, Grégoire MC. Correction of Partial-Volume Effect for PET Striatal Imaging: Fast Implementation and Study of Robustness. *J Nucl Med* 2002; 43:1715–1726
6. Hajnal, J.V., Saeed, N., Soar, E.J., Oatridge, A., Young, I.R., Bydder, G.M., 1995. A registration and interpolation procedure for subvoxel matching of serially acquired MR images. *J Comput Assist Tomogr* 19, 289-296.
7. Joshi, A., Koeppe, R.A., Fessler, J.A., 2009. Reducing between scanner differences in multi-center PET studies. *Neuroimage* 46, 154-159.
8. Klunk WE, Engler H, Nordberg A, Wang,Y, Blomqvist G, Holt DP, Bergstrom M, Savitcheva I, Huang GF, Estrada S, Ausen B, Debnath ML, Barletta J, Price JC, Sandell J, Lopresti BJ, Wall A, Koivisto P, Antoni G, Mathis CA, Langstrom B. Imaging brain amyloid in Alzheimer's disease with Pittsburgh Compound-B. *Ann Neurol* 2004; 55, 306-319.
9. Klunk WE, Koeppe RA, Price JC, Benzinger TL, Devous MD Sr, Jagust WJ, Johnson KA, Mathis CA, Minhas D, Pontecorvo MJ, Rowe CC, Skovronsky DM, Mintun MA. The Centiloid Project: Standardizing quantitative amyloid plaque estimation by PET. *Alzheimer's & Dementia* 2015; 11(1):1-15.e4.
10. Logan J, Fowler AH, Volkow ND. Distribution volume ratios without blood sampling from graphical analysis of PET data. *J Cereb Blood Flow Metab* 1996; 16:834–840.
11. Lopresti BJ, Klunk WE, Mathis CA, Hoge JA, Ziolko SK, Lu X, Meltzer CC, Schimmel K, Tsopelas ND, DeKosky ST, Price JC. Simplified quantification of Pittsburgh Compound B amyloid imaging PET studies: a comparative analysis. *J Nucl Med* 2005; 46:1959-1972.
12. Marcus, DS, Archie, KA, Olsen, T, Ramaratnam, M. The open source neuroimaging research enterprise. *J. Digital Imaging* 2007; 20:130-138.
13. McCormick LM, Ziebell S, Nopoulos P, Cassell M, Andreasen NC, Brumm M. Anterior Cingulate Cortex: An MRI-based parcellation method. *NeuroImage* 2006; 32:1167-1175.
14. Mintun MA, LaRossa GN, Sheline YI, Dence CS, Lee SY, Mach RH, Klunk WE, Mathis CA, DeKosky ST, Morris JC. [11C]PIB in a nondemented population: Potential antecedent marker of Alzheimer disease. *Neurology* 2006; 67:446-452
15. Shruti, M, Gordon BA, Su, Y, Christensen, J, Friedrichsen, K, Jackson K, Hornbeck, R, Balota DM, Cairns, N, Ances, B, Morris, JC. Benzinger TLS. Tau PET imaging in preclinical Alzheimer's Disease: Classifying tau Positivity. *NeuroImage* 2017; 161: 171-178
16. Morris, JC, Roe, CM, Xiong, C, Fagan, AM, Goate, AM, Holtzman, DM, Mintun, MA. APOE predicts amyloid-beta but not tau Alzheimer pathology in cognitively normal aging. *Ann Neurol* 2010; 67:122-131.
17. Ostrowitzki S, Deptula D, Thurfjell L, Barkhof F, Bohrmann B, Brooks DJ, Klunk WE, Ashford E, Yoo K, Xu ZX, Loetscher H, Santarelli L. Mechanism of amyloid removal in patients with Alzheimer disease treated with gantenerumab. *Arch Neurol* 2011; 69:198-207

18. Price TR, Manolio TA, Kronmal RA, Kittner SJ, Yue NC, Robbins J, Anton-Culver H, O'Leary DH. Silent brain infarction on magnetic resonance imaging and neurological abnormalities in community-dwelling older adults. The Cardiovascular Health Study. CHS Collaborative Research Group. *Stroke*. 1997;28(6):1158-64. PMID: 9183343.
19. Robb, R.A., Hanson, D.P., Karwoski, R.A., Larson, A.G., Workman, E.L., Stacy, M.C. Analyze: a comprehensive, operator-interactive software package for multidimensional medical image display and analysis. *Comput Med Imaging Graph* 1989; 13:433-454.
20. Rousset O, Ma Y, Evans A. Correction for partial volume effects in PET: principle and validation. *J Nucl Med* 1998; 39:904–11.
21. Rousset O, Zaidi H. Correction of partial volume effects in emission tomography. In: Zaidi H, ed- itor. Quantitative analysis of nuclear medicine images. New York: Springer; 2006. p. 236–271.
22. Rowland DJ, Garbow JR, Laforest R, Snyder AZ. 2005 Registration of [18F]FDG microPET and small-animal MRI. *Nucl Med Biol* 2005; 32:567-72
23. Sperling RA, Aisen PS, Beckett LA, Bennett DA, Craft S, Fagan AM, Iwatsubo T, Jack CR, Jr., Kaye J, Montine TJ, Park DC, Reiman EM, Rowe CC, Siemers E, Stern Y, Yaffe K, Carrillo MC, Thies B, Morrison-Bogorad M, Wagster MV, Phelps CH. Toward defining the preclinical stages of Alzheimer's disease: recommendations from the National Institute on Aging-Alzheimer's Association workgroups on diagnostic guidelines for Alzheimer's disease. *Alzheimer's & dementia*. 2011;7(3):280-92. PMID: 21514248; PMCID: PMC3220946
24. Su Y, D'Angelo GM, Vlassenko AG, Zhou GF, Snyder AZ, Marcus DS, et al. Quantitative Analysis of PiB-PET with FreeSurfer ROIs. *PLoS One* 2013;8(11):e73377. PMCID: 3819320
25. Su Y, Blazey TM, Snyder AZ, Raichle ME, Marcus DS, Ances BM, Bateman RJ, Cairns NJ, Aldea P, Cash L, Christensen JJ, Friedrichsen K, Hornbeck RC, Farrar AM, Owen CJ, Mayeux R, Brickman AM, Klunk W, Price JC, Thompson PM, Ghetty B, Saykin AJ, Sperling RA, Johnson KA, Schofield PR, Buckles V, Morris JC, Benzinger TL, Network DIA. Partial volume correction in quantitative amyloid imaging. *Neuroimage*. 2015;107:55-64. PMCID: 4300252.
26. Su Y, Blazey TM, Owen CJ, Christensen JJ, Friedrichsen K, Joseph-Mathurin N, Wang Q, Hornbeck RC, Ances BM, Snyder AZ, Cash LA, Koeppe RA, Klunk WE, Galasko D, Brickman AM, McDade E, Ringman JM, Thompson PM, Saykin AJ, Ghetty B, Sperling RA, Johnson KA, Salloway SP, Schofield PR, Masters CL, Villemagne VL, Fox NC, Forster S, Chen K, Reiman EM, Xiong C, Marcus DS, Weiner MW, Morris JC, Bateman RJ, Benzinger TL, Dominantly Inherited Alzheimer N. Quantitative Amyloid Imaging in Autosomal Dominant Alzheimer's Disease: Results from the DIAN Study Group. *PLoS One*. 2016;11(3):e0152082. PMCID: PMC4807073.
27. Su Y, Flores S, Hornbeck RC, Speidel B, Vlassenko AG, Gordon BA, Koeppe RA, Klunk WE, Xiong C, Morris JC, Benzinger TLS. Utilizing the Centiloid scale in cross-sectional and longitudinal PiB PET studies. *NeuroImage: Clinical* 19 (2018): 406-416.
28. Su Y, Flores S, Wang G, et al. Comparison of Pittsburgh compound B and florbetapir in cross-sectional and longitudinal studies. *Alzheimers Dement (Amst)*. 2019;11:180–190.
29. Talairach J, Tournoux P. Co-planar Stereotaxic Atlas of the Human Brain: 3-D Proportional System: An Approach to Cerebral Imaging. Stuttgart, Germany: Thieme Medical Publishers; 1988.
30. Wahlund LO, Barkhof F, Fazekas F, Bronge L, Augustin M, Sjogren M, Wallin A, Ader H, Leys D, Pantoni L, Pasquier F, Erkinjuntti T, Scheltens P. A new rating scale for age-related white matter changes applicable to MRI and CT. *Stroke*. 2001;32(6):1318-22. PMID: 11387493.
31. Accorsi R, Adam LE, Werner ME, and Karp JS. Optimization of a fully 3D single scatter algorithm for 3D PET. *Phys Med Bio* 2004; 49: 2577-2598.